A spatial model of germinal center reactions: Cellular adhesion based sorting of B cells results in efficient affinity maturation

Can Keşmir and Rob J. De Boer
Theoretical Biology group, Utrecht University,
Padualaan 8, 3584-CH Utrecht, The Netherlands.
April 9, 2001

Corresponding Author:
Dr. Can Keşmir
Department of Theoretical Biology, Utrecht University,
Padualaan 8, NL-3584-CH Utrecht, The Netherlands.
Email: C.Kesmir@bio.uu.nl
Fax: +31 30 2513655
Keywords:
germinal centre reactions; affinity maturation; cellular adhesion; spatial model
Running title:

Affinity maturation in a spatial germinal center model

Abstract

Affinity maturation during immune responses to T-dependent antigens occurs in germinal centers (GC). In GCs antigen specific B cells undergo rounds of somatic mutations that alter their affinity. High affinity mutants take over GCs very soon after they appear; the replacement rate is as high as 4 per day [43]. To gain more insight into this selection process, we present a spatial model of GC reactions, where B cells compete for survival signals from follicular dendritic cells (FDC). Assuming that high affinity B cells have increased cellular adhesion to FDCs, we obtain an affinity based sorting of B cells on the FDC. This sorting results in a *winner-takes-all* behavior. By comparing our sorting model with "affinity-proportional selection models", we show that a *winner-takes-all* selection is required to account for the fast rates at which high affinity mutants take over GCs.

1 Introduction

The antibody response to T-cell dependent antigens matures in germinal centers [31], where B cells undergo extensive proliferation and differentiation [28, 30, 50]. The GC environment provides signals to the B cells, causing them to switch on a hypermutation mechanism that alters their affinity [4, 19, 22, 51–53]. The high mutation rate amounts to roughly 10^{-3} per base-pair per division [3], i.e. each B cell is expected to produce approximately one mutant per cell division. Under such conditions, a high affinity clone would suffer mutational decay unless it is subject to very strong selection. Selection takes place in two stages. First, mutated B cells compete for antigen bound to FDCs [18, 42]. Second, they compete for T cell help [10, 27, 32, 54].

The strong selection in GCs results in an *all-or-none* behavior, i.e. GCs either contain hardly any high affinity cells, or they are almost completely taken over by high affinity mutants [2, 43]. Radmacher *et al.* calculated the replacement rate of a high affinity mutant (having 10-fold increased affinity) to be almost 4 per day [43]. Since the estimated maximum proliferation rate for any GC B cells is also 4 per day [30], the growth rate (or fitness) of the germ line B cells seems to drop to zero when the first high affinity mutants appear. we can make this argumentation more precise by developing a simple affinity proportional selection model.

A simple affinity-proportional selection model

Consider an established GC with a steady-state germ-line B cell population G proliferating at a rate of 4 per day. The germ-line B cells have an affinity K that influences their proliferation rate ρ, or their death rate δ. We assume that the total number of B cells in the GC, T, remains approximately constant when a mutant B cell M, with affinity κ ($\kappa > K$), takes over, i.e., $G + M = T$. First, consider a model where the affinity determines only the proliferation rates, i.e., B cells die at a constant rate, δ, independent of their affinity. For the germ-line B cells, G, we write:

$$\frac{\mathrm{d}G}{\mathrm{d}t} = (\rho(K) - \delta)G, \tag{1}$$

where $\rho(K) = \delta \simeq 4$ per day, and for the mutant, M, we write:

$$\frac{\mathrm{d}M}{\mathrm{d}t} = (\rho(\kappa) - \delta)M. \tag{2}$$

When germ-line B cells are in a steady-state, i.e. $\mathrm{d}G/\mathrm{d}t = 0$, $\delta = \rho(K)$. Since we consider the case where germ-line cells and mutants differ only in their proliferation rate, we can substitute $\delta = \rho(K)$ in Eq.(2) to obtain $\mathrm{d}M/\mathrm{d}t = (\rho(\kappa) - \rho(K))M$. Hence the mutant expands at a rate defined by the difference in the proliferation rates (which is an obvious result of population genetics [34]). The observed replacement rate of 4 per day therefore requires that $\rho(\kappa) \simeq 8$ per day, which is unrealistically fast. Moreover, if

the next mutant with further increased affinity ($\kappa' > \kappa$) were also to take over at a rate of 4 per day, it would need to have $\rho(\kappa') = 12$ per day, which is even more unrealistic.

As an alternative model we assume that the affinity determines the death rates. Then:

$$\frac{\mathrm{d}G}{\mathrm{d}t} = (\rho - \delta(K))G \tag{3}$$

with $\rho = \delta(K) \simeq 4$ per day in the steady-state, and

$$\frac{\mathrm{d}M}{\mathrm{d}t} = (\rho - \delta(\kappa))M = (\delta(K) - \delta(\kappa))M. \tag{4}$$

Thus, in such a situation the mutant expands at a rate defined by the difference in the death rates. To obtain a replacement rate of 4 per day with $\delta(K) \simeq 4$ per day [11], one needs $\delta(\kappa) \simeq 0$. Thus, the mutant has to have an infinite lifetime, which is again unrealistic. Moreover, since the fitness cannot be improved any further beyond $\delta(\kappa) = 0$, this mutant cannot be taken over by new mutants with further increased affinities.

We conclude that to explain the *in vivo* data, we need a new mechanism that allows for stronger selection of high affinity mutants. We investigate a possible new selection mechanism by replacing the assumption of affinity-proportional death or proliferation rates by affinity based sorting of centrocytes on FDCs. We develop a spatial GC model in which B cells move, divide, mutate, and die. In this model B cells compete with each other for space (i.e. for survival signals) on the FDC surface. We obtain a spatial sorting of the B cells on the FDC if we assume that B cells with increased affinity have an increased cellular adhesion to FDC. This leads to a *winner-takes-all* selection because, by means of adhesion based cellular sorting [47], only the highest affinity B cells will contact the FDC and be rescued. The formalism used for our model was developed earlier for adhesion based cell sorting [12, 13], and is here extended with GC-specific cellular processes.

Many theoretical models of affinity maturation have been published in the last decade, e.g.[20, 21, 38, 39]. Previous models, although good at simulating the *average* affinity maturation, are poor at explaining the rapid take-over of mutants, i.e. the *all-or-none* behavior of individual GCs. The major reason for this is the affinity-proportional selection mechanism (see above). We compare our model to earlier models and show that with adhesion based cellular sorting we obtain much faster selection of a sequence of high affinity mutants.

2 Model

2.1 Biology of germinal centers

The primary humoral follicular immune response starts with the rapid expansion of 3–5 antigen-specific B blasts [16, 30]. Within 3 days B cell numbers exceed 10^3. This

rapid expansion is followed by differentiation: a certain fraction of blast cells (i.e. the centroblasts) remains in the cell cycle, downregulates its surface immunoglobulin, and creates the dark zone of the GC. The remaining blast cells (i.e. the centrocytes) move to the opposite pole of the FDC network, re-express their surface immunoglobulin, and create the light zone.

In a GC, B cells can alter their phenotypes. After a certain number of cell divisions centroblasts revert to the centrocyte phenotype [30]. Centrocytes do not proliferate, and die rapidly unless they are "rescued". The centrocytes receive the first survival signal when they form complexes with antigen on FDCs [23]. While dissociating from FDCs, the centrocytes take up some antigen, which is later presented to GC T cells to get the second (cognate) survival signal [7, 23]. A centrocyte is rescued if it wins both antigen driven and T cell driven selection. A rescued centrocyte exits the light zone, and either leaves the GC to become a memory or plasma cell, or recirculates back to the dark zone, where it restarts centroblast proliferation. Recent data suggest that the memory B cell population is generated throughout the GC reaction [44].

2.2 Basic principles of the model

To study the affinity maturation process, we use a hybrid cellular automata (CA) like the model introduced by Graner & Glazier [12, 13] (see the Appendix). This model has been used extensively for simulating cell sorting [36, 37], morphogenesis [14, 15] and for simulating all stages of *Dictyostelium discoideum* slugs [17, 33, 35, 46].

The space in which the GC simulations take place is a rectangular lattice of CA "sites". Each biological cell is simulated by a combination of connected lattice sites. A cell interacts with other cells and the medium according to predefined rules, dependent on the cell type (e.g. centrocyte, centroblast, FDC, or memory). In Figure 1 we show a sketch of the lattice, where two centrocytes with a high (brown) and a low (yellow) affinity are interacting with an FDC. During a single update a randomly chosen lattice site is replaced by a randomly chosen neighbor with a probability that depends on the change in surface energy that would be brought about by the update. Lattice sites inside a cell are never updated, because exchanging two sites within a cell does not change the state of the system. In the original model [12, 13], the surface energy is the sum of adhesion energies between cells of different types or medium (e.g. $J_{c,c}$, $J_{f,c}$, $J_{f,m}$, $J_{m,c}$ in Figure 1, and see the Appendix). To keep cells close to their target volume, an extra volume constraint term is added to the surface energy calculations. In the original model, a constant target volume is used, and this causes very fast cell growth when the space is not limited. To obtain slow cell growth, we set the target volume of a cell to a small value after cell division and then increase the target volume gradually (see also [14]). This means that, when the actual volume of a cell exceeds the target volume plus a threshold, the target volume is increased. This process is repeated until the target volume reaches a predefined maximum.

***** Please insert fig.1 about here *****

We extend the model by letting the cell adhesion between the centrocytes and the FDC depend partly on the affinity of centrocytes for the antigen on the FDCs (see Eq.(6) in the Appendix). The shaded area in Figure 1 shows the sites where affinity contributes to the cell adhesion. Thus, it is more advantageous for a high affinity cell to be in contact with the FDC than it is for a low affinity cell. As a result, high affinity centrocytes tend to replace low affinity centrocytes on the FDC surface. Thus, the chance that a low affinity centrocyte will come into contact with the FDC decreases with the number of high affinity centrocytes that are around. In Figure 2 we show a series of snap-shots from a simulation to demonstrate the affinity based cell sorting around the FDC.

***** Please insert fig.2 about here *****

2.3 Cellular processes implemented in the model

Simulations start with 6-8 seeder centroblasts. Before a centroblast can divide it has to grow to a certain fixed volume. Hence, the number of cell divisions in this spatial model depends on the empty space available. A centroblast converts to a centrocyte after a predefined time. In the sorting model this time remains independent of the centrocytes' affinity for the antigen.

Centrocytes need to interact with the FDC to be "rescued" from programmed cell death. We implement a chemotactic gradient towards the FDC to which only centrocytes respond [5]. This chemotactic gradient helps the centrocytes to find the FDC. Centrocytes compete with each other to gain access to the FDC surface. Once the centrocytes establish an FDC contact area, covering more than three lattice sites, three being the predetermined threshold, they start receiving survival signals. A centrocyte is rescued after it has accumulated a certain amount of survival signals, i.e. after being in contact with the FDC for a minimum amount of time. The affinity of a centrocyte does not influence the amount of survival signals it needs to accumulate to be rescued; the affinity only affects the sorting. By a stochastic chance a rescued centrocyte either becomes a memory cell, or reverts to the centroblast phenotype. Because we assume that only centrocytes have a strong adhesion to the FDC [40], they dissociate from the FDC upon changing their phenotype. Model memory cells leave the GC rapidly, because they are repelled by the chemotactic signals secreted by the FDC. Thus, a memory cell has little influence on our GC dynamics. The lifetimes of centrocytes are predefined (some noise is added in order to prevent synchronization). In the sorting model the lifetime of a centrocyte remains independent of its affinity for the antigen. If a centrocyte does not accumulate enough survival signals during its lifetime, it dies.

A B cell's affinity for the antigen can change by somatic mutation. We group B cells (both centrocytes and centroblasts) into a small number of affinity classes, where all cells in affinity class i are assumed to have similar affinity for the antigen. Germ-line antigen-specific B cells are in affinity class 0. Somatic mutation is implemented as a stochastic process during cell division. Following a somatic mutation a B cell from

affinity class i can either switch to class $i+1$, i.e. achieve higher affinity, or switch to class $i-1$, i.e. get lower affinity. The former, i.e. obtaining higher affinity, is less likely than the latter.

2.4 The parameters

From the selection point of view, the crucial parameters of the model are the minimum interaction time needed to rescue a centrocyte and the contribution that affinity makes to cell adhesion. These parameters are discussed in detail in section 3.3. The mutation rate, the probability of getting an advantageous mutation, and the lifetime of centroblasts in combination influence the *all-or-none* behavior, and are discussed in section 3.2. The probability p_r with which a rescued centrocyte will become a centroblast, influences the size of a GC reaction. Varying the recycling probability between 0.2 to 0.6, for example, changes the GC size three fold. When $p_r = 0$, the influx of B cells to the centroblast compartment is zero, and the GC reaction cannot be maintained.

To convert simulation time steps into real time, we measure the average time that elapses between cell divisions in initial phases of the simulation, i.e. when the space is not yet a limiting factor. In experimental GC reactions centroblasts have been shown to divide once every 6-7 hrs [30]. Using this estimate, 3500 time steps in our simulations correspond to a single day (i.e., each time step corresponds to approximately 25 seconds).

Some parameter values have not been well established experimentally. They have been tuned within reasonable limits to obtain a model behavior that seems realistic (see Table I).

***** Please insert Table I about here *****

3 Results

We investigate whether the affinity based sorting of centrocytes around FDCs (see section 2.2) allows for fast selection of high affinity mutants. First we ask whether fast take-over rates can be reached in biologically realistic parameter regimes. Thus we neglect mutation and explicitly introduce high affinity mutants in a sequential manner into established GC reactions to see how fast they take over. This yields the take-over rate for a single high affinity mutant in a population of low affinity cells.

The simulations start with germ-line affinity seeders, i.e. with B cells belonging to affinity class 0. When the GC reaction consisting of germ-line affinity B cells approaches steady state, we introduce the first high affinity mutant from affinity class 1. Due to the stochastic nature of the model, a single high affinity mutant has a "probability" of taking over a GC reaction. For instance, if the mutant fails to reach the FDC, it will not be selected. Following the terminology introduced by Radmacher *et al.*, we define a founder mutant as the first mutant in a key lineage which ultimately accounts

for domination of the GC [43]. If the first mutant fails to become a founder mutant, we later introduce another mutant of the same affinity class. This process is repeated until one of the mutants becomes the founder mutant, and the GC reaction is dominated by cells from affinity class 1. Next the same procedure is repeated for a mutant of the next affinity class. The results of such a simulation are shown in Figure 3A. The low plateau prior to the fast increase in cell numbers for each affinity class corresponds to the waiting time for the founder mutant; the mutants introduced in this initial phase fail to take over a GC reaction. By the end of the four-week period, the GC is populated by B cells of affinity class five. Note from the cell numbers on the vertical axis that the model GC is 10-fold smaller than a typical biological GC [16]. It would be possible to do larger simulations having realistic B cell numbers if the number of FDCs and the lattice size were to be increased.

Affinity-proportional selection mechanisms (see e.g. Eq.(2)) can easily be implemented in our model by i) excluding the affinity from the adhesion calculation, (i.e., by setting bA to zero in Eq.(6)), and ii) making the average lifetime of centroblasts, or centrocytes, inversely proportional to their affinity. In such a model a high affinity mutant would either have a longer centroblast lifetime (i.e., a higher chance of having more offspring), or it would have a longer centrocyte lifetime (i.e., a higher chance of receiving survival signals from the FDC). In Figure 3B we show a typical time plot of a model in which the life span of centrocytes increases fold-wise with affinity (i.e. proportional to 2^A, where A is the affinity). Figure 3 shows that the sorting model achieves better affinity maturation in one month than does an affinity-proportional selection model.

***** Please insert fig.3 about here *****

As the model is highly stochastic, we run 40 simulations, each initialized with different random seeds so that we can compare different selection mechanisms. For each affinity class we determine the founder mutant. We define the take-over rate of the founder mutants as follows (see [34]). For the period where 10 to 90% of GC B cells are offspring of the founder mutant, we do a linear regression on the fraction of high affinity cells. The slope of this fit defines the take-over rate of that mutant. The results are depicted in Figure 4. In the sorting model (squares) the replacement rate depends only on the affinity differences, not on the absolute affinity values. For example, a mutant from affinity class three replaces B cells from affinity class two at the same rate as a class one mutant replaces germ-line affinity cells. We compare the sorting model with four different affinity-proportional selection models. In the four models the lifetimes of the centrocytes, or centroblasts, increase either proportionally, or fold-wise (i.e. in powers of 2), with the affinity. The lifetimes used in these models are given in Figure 4B. In the sorting model, a centrocyte has an average lifetime of 6h, and a centroblast lives on average for 12h.

The replacement rates in the affinity-proportional selection models are much slower than those in the sorting model (see Figure 4). The difference in take-over rates reached by the sorting model and the affinity-proportional selection models increases with the affinity classes. This is due to the fact that in the affinity-proportional selection models

cells becomes very long lived when the affinity increases. Thus replacing them takes a long time. The results in Figure 4A suggest that the centrocyte lifetime plays a larger role in affinity maturation than the centroblast lifetime. This is because longer centrocyte lifetimes increase the chance of receiving survival signals. Long-living centroblasts might get more offspring; however, this does not directly increase the take-over rates.

***** Please insert fig.4 about here *****

3.1 Waiting time for founder mutants

The cautious analysis by Radmacher et al. [43] shows that high affinity mutants appear much later than is expected from known mutation rates and mutation motifs. For the anti-(4-hydroxy-3-nitrophenyl) acetyl (NP) response the waiting time for the key mutant with one mutation at position 33 is 8.3 days [43]. This waiting time strongly contradicted with the expected time of 2.3 days. Apparently an average of 2.6 mutants arise, but do not take root in GCs before the *founder* mutant arrives. Radmacher *et al.* suggested several mechanisms that might cause the failure of early high affinity mutants, e.g. a low chance of finding the right T cell, or fast emigration from the GC.

The cellular processes in our hybrid GC are highly stochastic, which might explain why not every high affinity mutant takes over a GC. If so, one need not consider mechanisms that affect early high affinity mutants only. Many processes which take place in our model are stochastic. How many offspring a high affinity mutant generates depends on where and when in the life cycle the advantageous mutation occurs. A centroblast acquiring an affinity-increasing mutation late in the life cycle is expected to have a small number of offspring before becoming a centrocyte. Additionally, the space available around a centroblast affects the number of offspring it gets. The chance of reaching the FDC and being rescued is proportional to the number of offspring (i.e. clone size).

To study the waiting time of founder mutants we ran 40 simulations without a mutation schedule. We introduced high affinity mutants one after the other, until one of them became the founder mutant. In Figure 5 we plot the fraction of simulations in which the first, second, third, etcetera, high affinity mutants becomes the founder mutant. The mean waiting time for the founder mutant in the sorting model is 2.6 mutants, which is in good agreement with the calculations of Radmacher et al. [43]. The stochastic effects are less prominent in the affinity-proportional selection models. For example, in these models the fitness advantage of a high affinity mutant is independent of where in the GC the mutation takes place. Thus, the waiting time for the founder mutants is much shorter here; on average it is 1.1 mutant (see Figure 5). This difference in the waiting time is not sensitive to the parameters used (results not shown).

***** Please insert fig.5 about here *****

3.2 *All-or-none* behavior

GCs induced during immune responses to the haptens rarely contain both high and low affinity B cells [43]. Indeed an *all-or-none* behavior is observed, i.e., a GC is either dominated by a high affinity mutant or does not contain any high affinity mutant at all. In Figure 6A we plot the available data for the anti-NP [43] and anti-2-phenyl-oxazolone (phOx) [2, 55] responses. About 60% of the GCs analyzed have no high affinity mutants at all. There are very few mixed GCs, and the remaining GCs have high affinity mutants only.

To test whether the sorting model is able to simulate such an *all-or-none* behavior, we now allow cells to mutate during cell division. The probability of getting an advantageous mutation is set to 0.3%, which is the same as in the experimental systems. We again run 40 simulations and the distribution of high affinity mutants in the model GCs is shown in Figure 6B. Although the agreement between the experimental and simulation results is striking, the simulation results have to be interpreted with some caution. Since our model GC contains only 10% of the cells of a real GC, the stochastic effects are probably too large in our model. We are currently working on a 3-dimensional model, i.e. with larger GCs, to study this matter further. The results depicted in Figure 6B can only be obtained if the proliferation, mutation and selection cycle is short. The parameters we use allow centroblasts to have on average two cell divisions before converting to a centrocyte. If the centroblasts make several cell divisions without being selected, they accumulate disadvantageous mutations. This results in very poor affinity maturation, i.e. almost all GCs contain low affinity cells. In these simulations we assume that the expressed mutation rate per cell genome per division is 0.25. If cells mutate faster, it is again hard to maintain any GCs with high affinity mutants because of mutational erosion.

***** Please insert fig.6 about here *****

3.3 Crucial parameters

Only recently, few of the molecules regulating the adhesion between a B cell and an FDC [1, 40] have been identified. Thus, there have been no good estimates of the contribution of the affinity to the adhesion energy in the literature on B cells, at least to our knowledge. In other words, the value bA in Eq.(6) of the Appendix is not known. The results in Figure 7A depict the average replacement rate in five simulations for a range of bA values. We plot the replacement rates of a class one mutant in a GC established by germ-line affinity B cells (Figure 4A implies that the replacement rates should be the same for higher affinity mutants). When the affinity makes a small contribution to the adhesion, i.e. for low values of bA, the take-over is slow. This parameter regime results in mixed GCs, rather than the *winner-takes-all* behavior. Once bA is sufficiently large, e.g. $bA > 8$, increasing bA does not affect the replacement rates drastically. When the bA value becomes very large, the cellular adhesion overrules the volume constraints, which results in non-circular cells.

Another crucial parameter of the model is the minimum interaction time with the FDC required for rescuing a centrocyte. In the model we assume that the minimum interaction time is independent of the affinity. Obviously, if this time is very short, high affinity cells spend very little time on the surface of the FDC and can hardly block the survival signals for the other cells. The effect of this parameter on the replacement rate is shown in Figure 7B. Short interaction times result in very low replacement rates. The *winner-takes-all* behavior is realized only when the survival signals are delivered over a few hours, which is in agreement with *in vivo* estimates for this parameter [31].

***** Please insert fig.7 about here *****

4 Discussion

Two processes bring about efficient affinity maturation of humoral immune responses. First, the hypermutation mechanism has to generate a large number of mutations and second, mutants that encode higher affinity antibodies have to be selected efficiently [43]. In the earlier models of affinity maturation, the mechanism for efficiently selecting the high affinity mutants is typically proportional to their affinity, either via increased proliferation rates or via decreased apoptosis rates of high affinity cells [21, 38]. We have shown that in biologically reasonable parameter regimes these mechanisms are not able to explain the observed rapid replacement of low affinity cells (see Section 1). To solve this problem we proposed a novel mechanism where B cells sort on FDC surface according to their affinities. We have shown that such a mechanism results in a *winner-takes-all* behavior (see Figure 4).

In our model the replacement rate (see Figure 4) is lower than the observed 4 per day [43]. One explanation for this is the following: For converting a simulation time step to real time, we adopted a "conservative" approach and we measured how long the cell division takes in the early phase of the simulations (when the space is not yet a limiting factor). Using this value we calculated that each time step in the model corresponds to 25 seconds in real time. However, later in the simulations, when a GC is filled with B cells, the centroblasts division rate slows down due to spatial competition. On average the division rate is 3-4 times slower than during the early phase. Using the later cell division time, a simulation time step would correspond to 6 seconds, which results in replacement rates close to 4 per day (results not shown). The main result in Figure 4 is the fact that under the *same* conditions, e.g. where cells compete for space and are moving with the same speed, the affinity based cell sorting produces faster take-over rates than the affinity-proportional selection mechanisms.

T cells in the GC also play a role in the selection of high affinity mutants [10, 27, 32, 54]. Our model focuses on an FDC-based selection of mutants. However, a T cell-based selection would be different from an FDC based selection. FDCs are big stationary cells, whereas T cells are small and mobile. In a spatial model, these differences might play a role. In an FDC-based selection, the limiting factor, i.e. space on the FDC surface,

is always constant. This is not the case for T cell-based selection, especially if T cells proliferate after interacting with high affinity B cells.

Somatic mutations can take place either during cell division [8, 45] or during transcription, i.e., when the cell starts to re-express surface immunoglobulin (converting to the centrocyte phenotype) [41, 48]. Here we implement the mutations during cell division. In a recent mathematical model it has been shown that mutations during the transcription phase result in better affinity maturation [39]. We observe this in our simulations too: if affinity altering mutations occur during the transcription phase, the *all-or-none* behavior of Section 3.2 becomes more pronounced (results not shown).

It is difficult to verify experimentally how much a B cell's affinity for antigen contributes to its adhesion to FDC. However, we show in Figure 7A that the precise value of this contribution is not important, provided it plays a sufficient role. To demonstrate that high affinity cells have significantly higher adhesion to FDC than low affinity cells would be enough evidence to support for an adhesion-based selection mechanism. Some other simulation results can be tested more easily. For example, in Figure 7B we show that the minimum interaction time needed to receive survival signals should affect the efficiency of affinity maturation. Some molecules like 8D6 Ag [26] were shown to transmit survival/growth signals to B cells. Experiments with knock-out (or knock-in) animals where the density of the survival signals decreases (or increases) would allow one to test this prediction. We show that the current estimates of the minimum interaction time, amounting to a few hours [31], give rise to efficient affinity maturation (see Figure 7B).

Finally, the *winner-takes-all* behavior is not limited to competition of B cell mutants. Early in GC reactions there is also very strong competition between seeders [9]. Furthermore, post-GC antibody-forming cells in the bone marrow may compete directly for activation by antigen. There is good evidence that this process plays a major role in the post-GC maturation of humoral responses [49]. Winner-takes-all behavior is also observed in many other ecological systems (see e.g., Krause [24] for a review on lek mating systems).

Acknowledgements

This work was initiated by Berend Snel. This paper has benefited greatly from critical comments by Ludo Pagie, Vincent DeTours, José A. M. Borghans and Paulien Hogeweg. CK is supported by grant 809.37.009 of the Dutch Science Foundation.

References

[1] Airas, L. and Jalkanen, S. (1996) , *Blood* **88**, 1755

[2] Berek, C., Berger, A., and Apel, M. (1991) , *Cell* **67**, 1121

[3] Berek, C. and Milstein, C. (1987) , *Immunol. Rev.* **96**, 23

[4] Betz, A. G., Neuberger, M. S., and Milstein, C. (1993) , *Immunol. Today* **14**, 405

[5] Bouzahzah, F., Antoine, N., Simar, L., and Heinen, E. (1996) , *Res. Immunol.* **147**, 165

[6] Brachtel, E. F., Washiyama, M., Johnson, G. D., Tenner-Racz, K., Racz, P., and MacLennan, I. C. (1996) , *Scand. J. Immunol.* **43**, 239

[7] Casamayor-Palleja, M., Khan, M., and MacLennan, I. C. (1995) , *J. Exp. Med.* **181**, 1293

[8] Cascalho, M., Wong, J., Steinberg, C., and Wabl, M. (1998) , *Science* **279**, 1207

[9] Chen, Z., Koralov, S. B., Gendelman, M., Carroll, M. C., and Kelsoe, G. (2000) , *J. Immunol.* **164**, 4522

[10] Choe, J., Li, L., Zhang, X., Gregory, C. D., and Choi, Y. S. (2000) , *J. Immunol.* **164**, 56

[11] Cohen, J. J., Duke, R. C., Fadok, V. A., and Sellins, K. S. (1992) , *Annu. Rev. Immunol.* **10**, 267

[12] Glazier, J. A. and Graner, F. (1993) , *PHYSICAL. REVIEW. E* **47**, 2128

[13] Graner, F. and Glazier, J. A. (1992) , *PHYSICAL. REVIEW. LETTERS.* **69**, 2013

[14] Hogeweg, P. (2000a) , *J. theor. Biol.* **203**, 317

[15] Hogeweg, P. (2000b) , *Artif. Life.* **6**, 85

[16] Jacob, J., Kassir, R., and Kelsoe, G. (1991) , *J. Exp. Med.* **173**, 1165

[17] Jiang, Y., Levine, H., and Glazier, J. (1998) , *Biophys. J.* **75**, 2615

[18] Kelsoe, G. (1996) , *Immunity* **4**, 107

[19] Kelsoe, G. (1999) , *Curr. Opin. Immunol.* **11**, 70

[20] Kepler, T. B. and Perelson, A. S. (1993a) , *Immunol. Today* **14**, 412

[21] Kepler, T. B. and Perelson, A. S. (1993b) , *J. Theor. Biol.* **164**, 37

[22] Klein, U., Goossens, T., Fischer, M., Kanzler, H., Braeuninger, A., Rajewsky, K., and Kuppers, R. (1998) , *Immunol. Rev.* **162**, 261

[23] Koopman, G., Keehnen, R. M., Lindhout, E., Zhou, D. F., De Groot, C., and Pals, S. T. (1997) , *Eur. J. Immunol.* **27**, 1

[24] Krause, J. (1994) , *Biol. Rev. Camb. Philos. Soc.* **69**, 187

[25] Kroese, F. G., Wubbena, A. S., Seijen, H. G., and Nieuwenhuis, P. (1987) , *Eur. J. Immunol.* **17**, 1069

[26] Li, L., Zhang, X., Kovacic, S., Long, A. J., Bourque, K., Wood, C. R., and Choi, Y. S. (2000) , *J. Exp. Med.* **191**, 1077

[27] Lindhout, E., Koopman, G., Pals, S. T., and De Groot, C. (1997) , *Immunol. Today* **18**, 573

[28] Liu, Y. J. and Banchereau, J. (1997) , *Semin. Immunol.* **9**, 235

[29] Liu, Y. J., Barthelemy, C., de Bouteiller, O., and Banchereau, J. (1994) , *Adv. Exp. Med. Biol.* **355**, 213

[30] Liu, Y. J., Zhang, J., Lane, P. J., Chan, E. Y., and MacLennan, I. C. (1991) , *Eur. J. Immunol.* **21**, 2951

[31] MacLennan, I. C. (1994) , *Annu. Rev. Immunol.* **12**, 117

[32] Manser, T., Tumas-Brundage, K. M., Casson, L. P., Giusti, A. M., Hande, S., Notidis, E., and Vora, K. A. (1998) , *Immunol. Rev.* **162**, 183

[33] Maree, A. F. and Hogeweg, P. (2001) , *PNAS* in press

[34] Maree, A. F., Keulen, W., Boucher, C. A., and De Boer, R. J. (2000) , *J. Virol.* **74**, 11067

[35] Maree, A. F., Panfilov, A. V., and Hogeweg, P. (1999) , *J. theor. Biol.* **199**, 297

[36] Mombach, J. C. and Glazier, J. A. (1996) , *PHYSICAL. REVIEW. LETTERS.* **76**, 3032

[37] Mombach, J. C., Glazier, J. A., Raphael, R. C., and Zajac, M. (1995) , *PHYSICAL. REVIEW. LETTERS.* **75**, 2244

[38] Oprea, M. and Perelson, A. S. (1997) , *J. Immunol.* **158**, 5155

[39] Oprea, M., Van Nimwegen, E., and Perelson, A. S. (2000) , *Bull. Math. Biol.* **62**, 121

[40] Pals, S. T., Taher, T. E., Van der Voort, R., Smit, L., and Keehnen, R. M. (1998) , *Cell. Adhes. Commun.* **6**, 111

[41] Peters, A. and Storb, U. (1996) , *Immunity* **4**, 57

[42] Przylepa, J., Himes, C., and Kelsoe, G. (1998) , *Curr. Top. Microbiol. Immunol.* **229**, 85

[43] Radmacher, M. D., Kelsoe, G., and Kepler, T. B. (1998) , *Immunol. Cell. Biol.* **76**, 373

[44] Ridderstad, A. and Tarlinton, D. M. (1998) , *J. Immunol.* **160**, 4688

[45] Rogerson, B., Hackett, Jr, J., Peters, A., Haasch, D., and Storb, U. (1991) , *EMBO. J.* **10**, 4331

[46] Savill, N. J. and Hogeweg, P. (1997) , *J. theor. Biol.* **184**, 229

[47] Steinberg, M. S. (1970) , *J. Exp. Zool.* **173**, 395

[48] Storb, U., Peters, A., Klotz, E., Kim, N., Shen, H. M., Kage, K., Rogerson, B., and Martin, T. E. (1998) , *Curr. Top. Microbiol. Immunol.* **229**, 11

[49] Takahashi, Y., Dutta, P. R., Cerasoli, D. M., and Kelsoe, G. (1998) , *J. Exp. Med.* **187**, 885

[50] Tarlinton, D. (1998) , *Curr. Opin. Immunol.* **10**, 245

[51] Wabl, M., Cascalho, M., and Steinberg, C. (1999) , *Curr. Opin. Immunol.* **11**, 186

[52] Wiens, G. D., Roberts, V. A., Whitcomb, E. A., O'Hare, T., Stenzel-Poore, M. P., and Rittenberg, M. B. (1998) , *Immunol. Rev.* **162**, 197

[53] Yelamos, J., Klix, N., Goyenechea, B., Lozano, F., Chui, Y. L., Gonzalez Fernandez, A., Pannell, R., Neuberger, M. S., and Milstein, C. (1995) , *Nature* **376**, 225

[54] Yellin, M. J., Sinning, J., Covey, L. R., Sherman, W., Lee, J. J., Glickman-Nir, E., Sippel, K. C., Rogers, J., Cleary, A. M., Parker, M., et al. (1994) , *J. Immunol.* **153**, 666

[55] Ziegner, M., Steinhauser, G., and Berek, C. (1994) , *Eur. J. Immunol.* **24**, 2393

5 Appendix

We define the surface energy as a Hamiltonian

$$H = \sum J_{cell,cell} + \sum J_{cell,m} - bA + \lambda(v - V)^2 + \mu C, \tag{5}$$

where the first term is due to dimensionless free energy bonds made with neighboring cells and the magnitude depends on both cell types [12, 13]. The bond energy between a cell and the medium is given by $J_{cell,m}$. All J values are positive. In addition to bond energies, we assume that the affinity of B cells, A, contributes to the total surface energy. Obviously, this is true only when a B cell expresses surface immunoglobulin and is in contact with the antigen, i.e.

$$b = \begin{cases} 1 & \text{when a centrocyte is in contact with an FDC} \\ 0 & \text{otherwise} \end{cases} \tag{6}$$

A cell would minimize its surface free energy best by shrinking to a volume of zero. Thus one adds a volume constraint (i.e. the fourth term in Eq.(5)) to the free energy calculations, so that each cell keeps its actual volume v close to its target volume V. The parameter λ defines the "inelasticity".

Finally, chemotactic signals affect the cell movement. We assume that only the FDC produces chemotactic signals [5], C. Each cell type has a certain sensitivity to chemotaxis (i.e. μ is a parameter that is cell-type dependent). We use a simple chemotactic gradient, that decreases linearly with the distance from the source.

ΔH is the change in H when a lattice site j is copied to i. This probability is defined as a Boltzmann distribution, i.e.:

$$p = \begin{cases} 1 & \Delta H < \theta = 0 \\ e^{-\Delta H/T} & \end{cases}$$

where T is the default mobility of cells. In the simulations reported here we use $T = 20$ and $\lambda = 0.1$.

Parameter or Initial Condition	Value	Ref.
Number of seeder cells per GC	6-8	[25]
Maximum proliferation rate of centroblast cells	3.5 day^{-1}	[30]
Average lifespan of centrocytes	6 hrs	[11]
Average lifespan of centroblasts	12 hrs	[29]
Contribution of affinity to cell adhesion (b, defined in Appendix)	10	
Minimum interaction time needed to rescue a centrocyte	3.5 hrs	
Probability of rescued centrocytes becoming a centroblast (p_r)	0.8	
Target volume for centroblasts and memory cells	40 sites	
Target volume for centrocytes (smaller than centroblasts)	30 sites	[6]
Expressed mutation rate per genome per division	0.25	
Probability of getting an advantageous mutation	0.03	

Table I: Initial conditions and parameter values

Figure legends

1. A sketch of the model formalism.The brown and yellow cells are high and low affinity centrocytes, respectively. The blue cell is the FDC. J values correspond to the different free energy bonds between cells and the medium. For each lattice site that is in contact with the medium or another cell, there is a corresponding J value. In the figure we have depicted only some of the J values. The affinity of a centrocyte influences its adhesion only in the FDC contact area (shaded).

2. A series of snap-shots from simulations. The first picture shows a GC populated by low affinity cells (yellow). At $t = 0$ a high affinity mutant is introduced (brown cell). At the end of the second day, half of the cells are of high affinity, but the FDC is largely covered by high affinity cells. This panel represents the typical affinity based sorting around the FDC. After 4 days the high affinity B cells dominate the GC reaction.

3. **A.** A typical simulation of the sorting model. A GC reaction starts with a few seeder cells with germ-line affinity. After the system has reached steady-state we introduce a single high affinity mutant. This process is repeated each time a GC contains only cells from a single affinity class. **B.** Similar simulations in a model where the centrocyte lifetime increases fold-wise with the affinity of the cell (i.e. the lifetime is proportional to 2^A, where A is the affinity of the cell).

4. Comparison of the sorting model with the affinity-proportional selection models. The replacement rate is calculated as explained in the main text. In the left panel, the replacement rates in different models are given (squares represent the sorting model). Four affinity-proportional selection models are compared with the sorting model: (i) the centroblast lifetime increases linearly with the affinity class of

the cell (stars), i.e. the lifetime is proportional to kA, where k is a constant and A is the affinity class of a cell, (ii) the centroblast lifetime increases fold-wise with the affinity class of the cell (triangles), i.e., the lifetime is proportional to 2^A, (iii) the centrocyte lifetime increases linearly with affinity (diamonds), and finally (iv) the centrocyte lifetime increases fold-wise with affinity (circles). The lifetimes of the cells in the different models are given in panel B. In the sorting model the affinity of a cell does not influence its lifetime, i.e., the average lifetime of centrocytes and centroblasts is 6 hrs and 12hrs, respectively. Each point is an average of 40 simulations, and the error bars give the standard deviations for each affinity class.

5. The fraction of GC simulations versus the affinity class of the founder mutant calculated over 40 simulations for each model. The mean number of mutants preceding the founder mutant is 2.6 in the sorting model and 1.1 in the affinity-proportional centrocyte lifetime model.

6. **A.** Distribution of high affinity cells in GCs analyzed for the anti-NP [43] and the anti-phOx [2, 55] response (total of 22 GCs). **B.** Distribution of high affinity cells in model experiments (total of 40 GCs). The simulations are run for 14 days, and the probability of getting an advantageous mutation is set to 0.3%. Up to 14 days the percentage of GCs not containing any high affinity mutants is higher, whereas after 14 days, more GCs contain high affinity mutants only.

7. **A.**The effect of the contribution of affinity to cellular adhesion, bA on B cell competition. **B.** The effect of the interaction time with FDCs on B cell competition. Each data point is the mean of five simulations, and the error bars show the standard deviation.

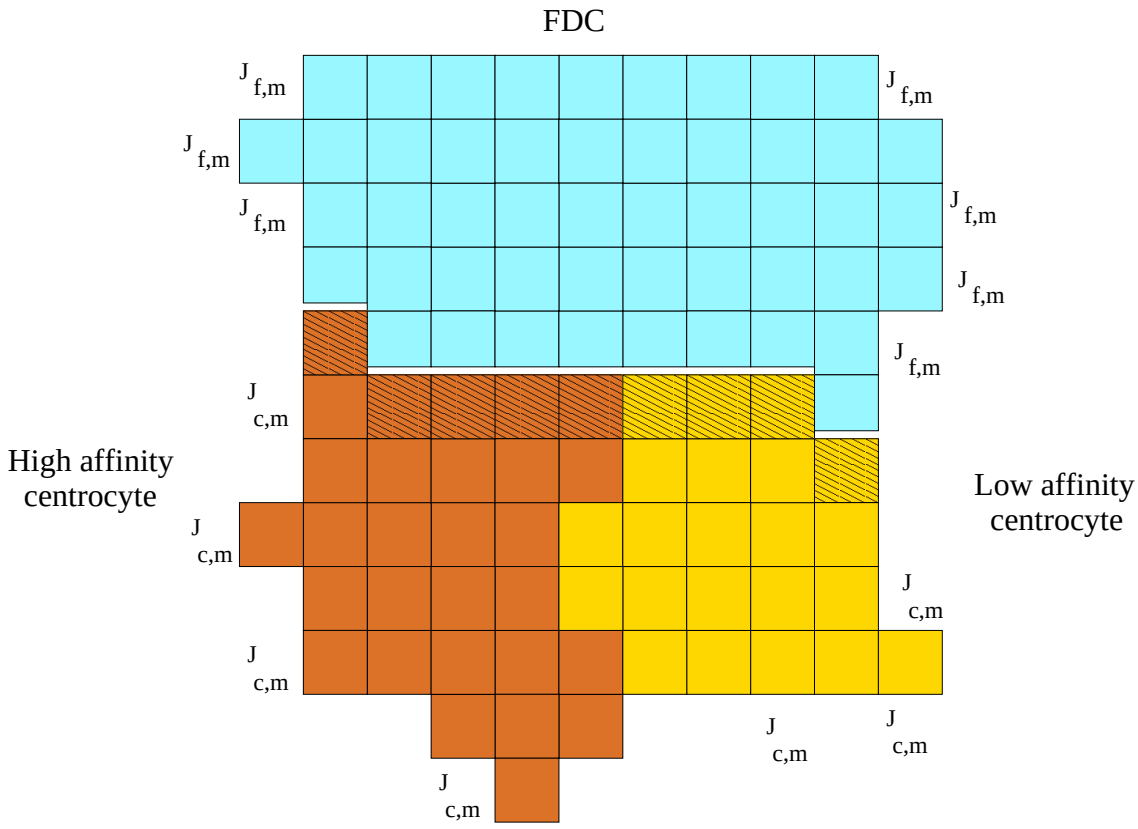
FDC
J f,m
J f,m
J f,m
J f,m
J f,m
J f,m
J c,m
High affinity centrocyte
Low affinity centrocyte
J c,m
J c,m
J c,m
J c,m
J c,m
J c,m

Figure 1:

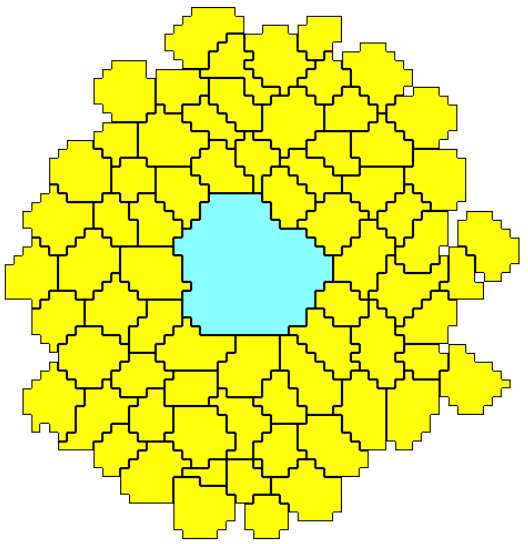

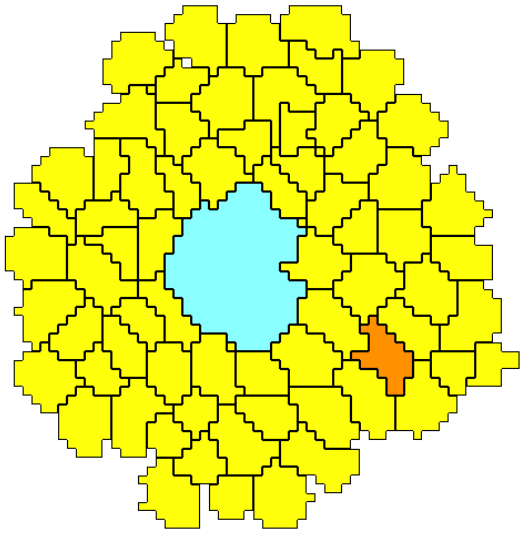

t=0

t=2 days

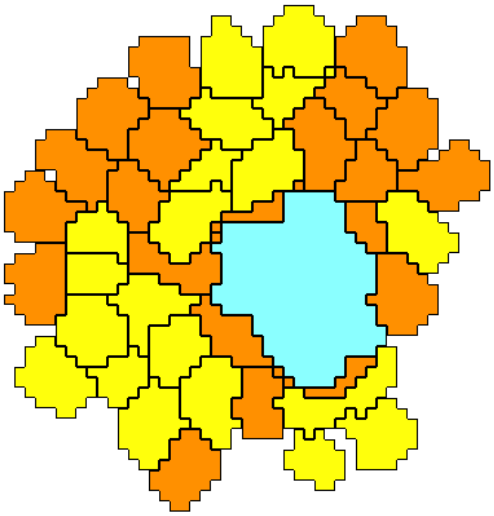

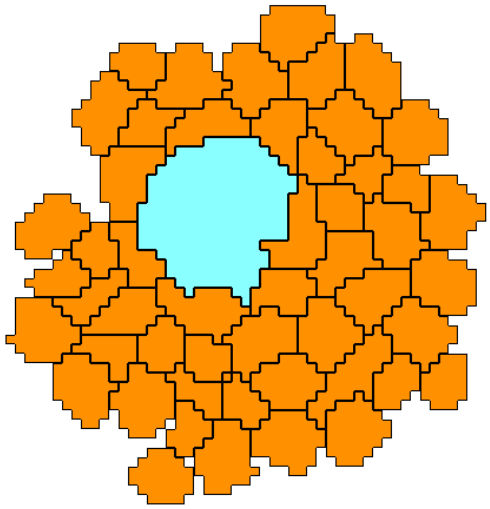

t=4 days

Figure 2:

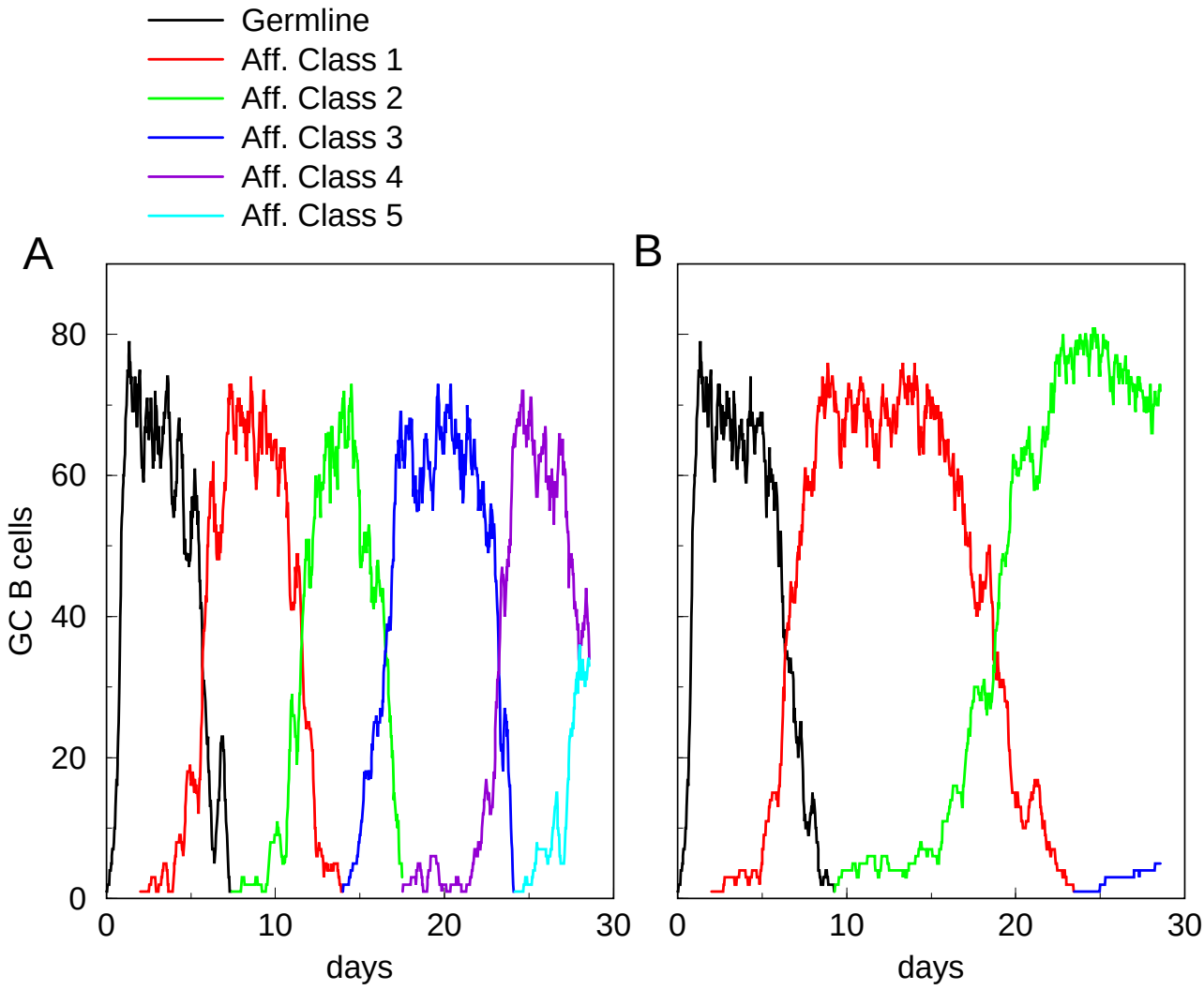
Germline
Aff. Class 1
Aff. Class 2
Aff. Class 3
Aff. Class 4
Aff. Class 5
A
B
GC B cells
0
20
40
60
80
0
10
20
30
days
0
10
20
30
days

Figure 3:

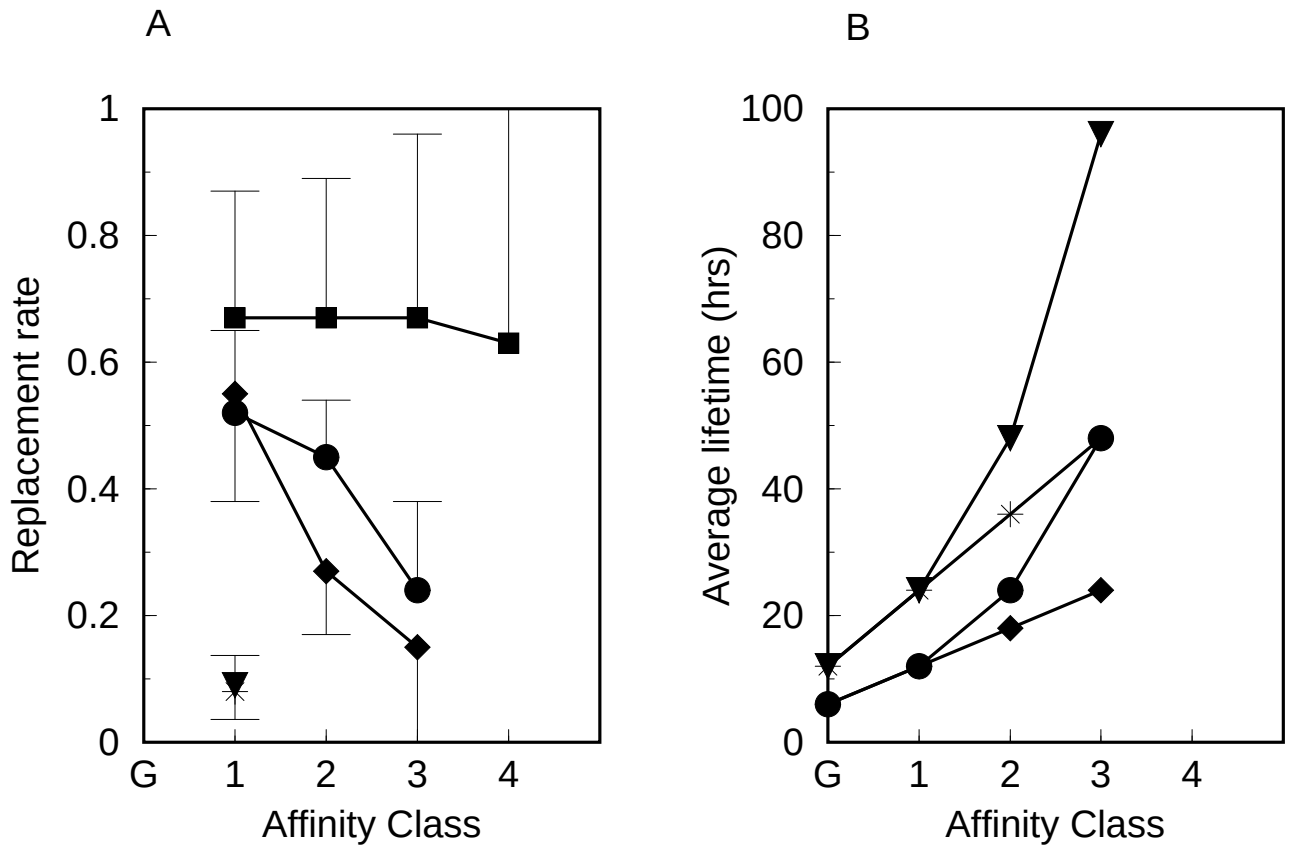
A
B
Replacement rate
Average lifetime (hrs)
Affinity Class
Affinity Class
G
1
2
3
4
0
0.2
0.4
0.6
0.8
1
20
40
60
80
100

Figure 4:

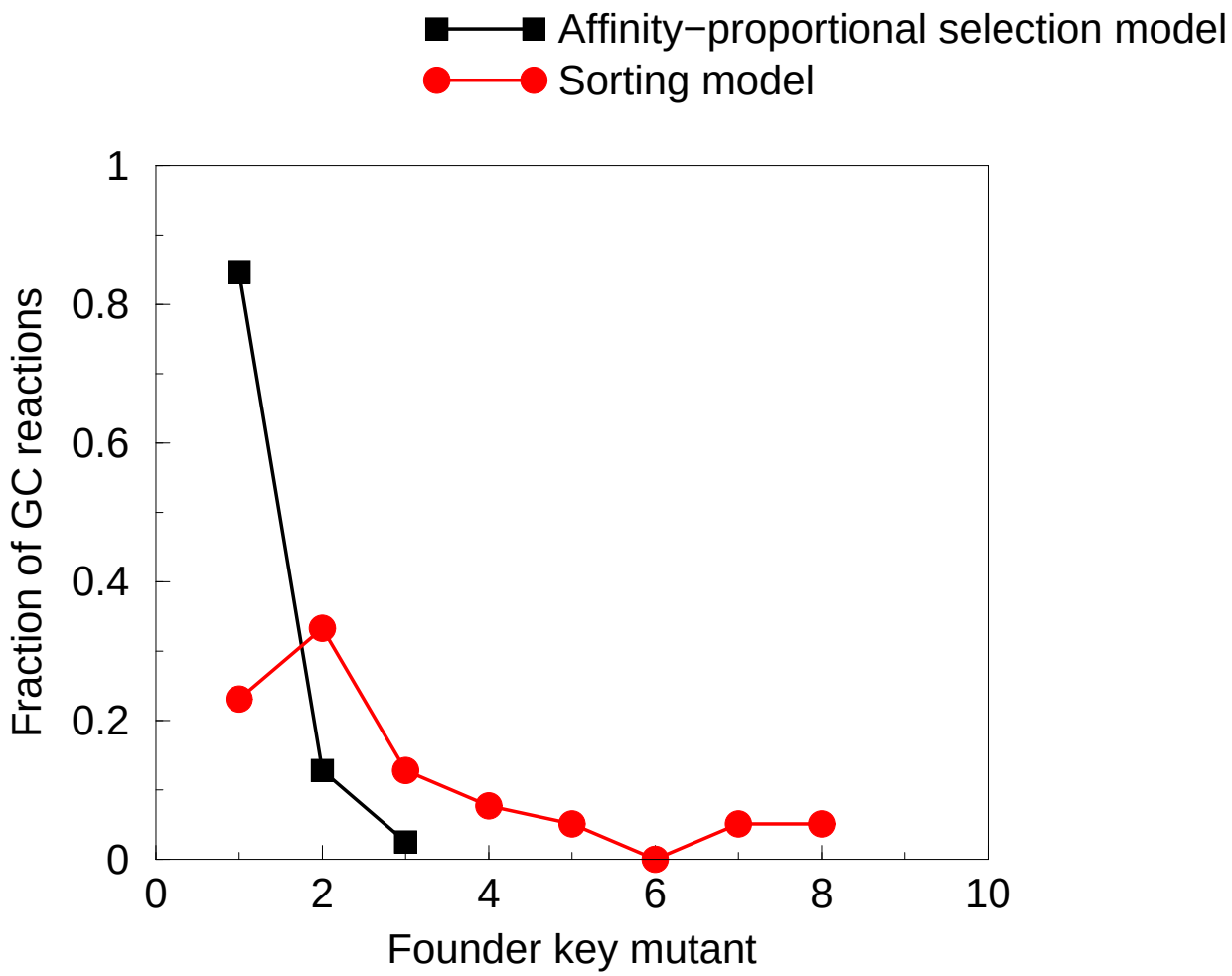
Affinity−proportional selection model
Sorting model
Fraction of GC reactions
1
0.8
0.6
0.4
0.2
0
0
2
4
6
8
10
Founder key mutant

Figure 5:

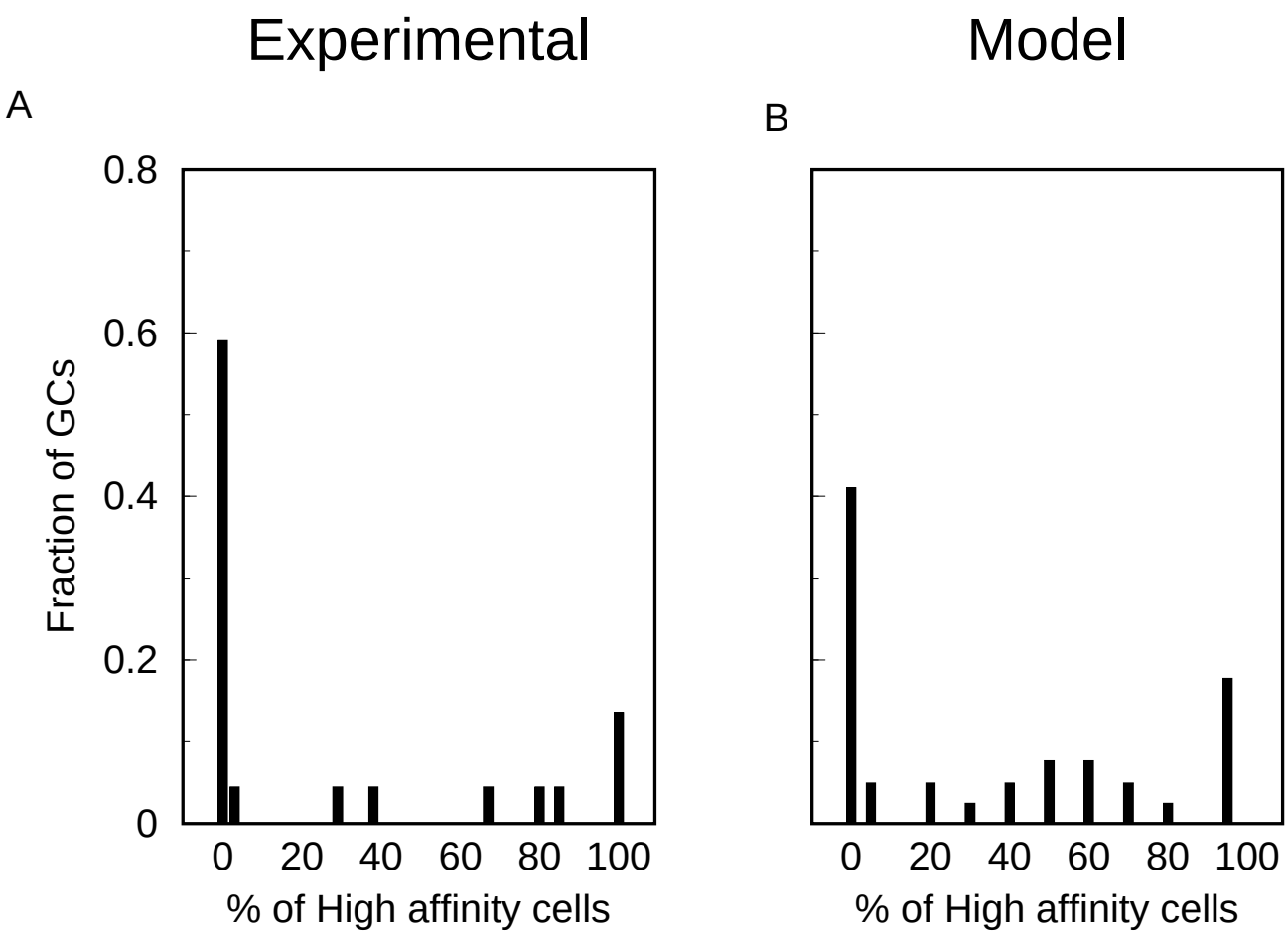
Experimental
Model
A
B
Fraction of GCs
0.8
0.6
0.4
0.2
0
0 20 40 60 80 100
% of High affinity cells
0 20 40 60 80 100
% of High affinity cells

Figure 6:

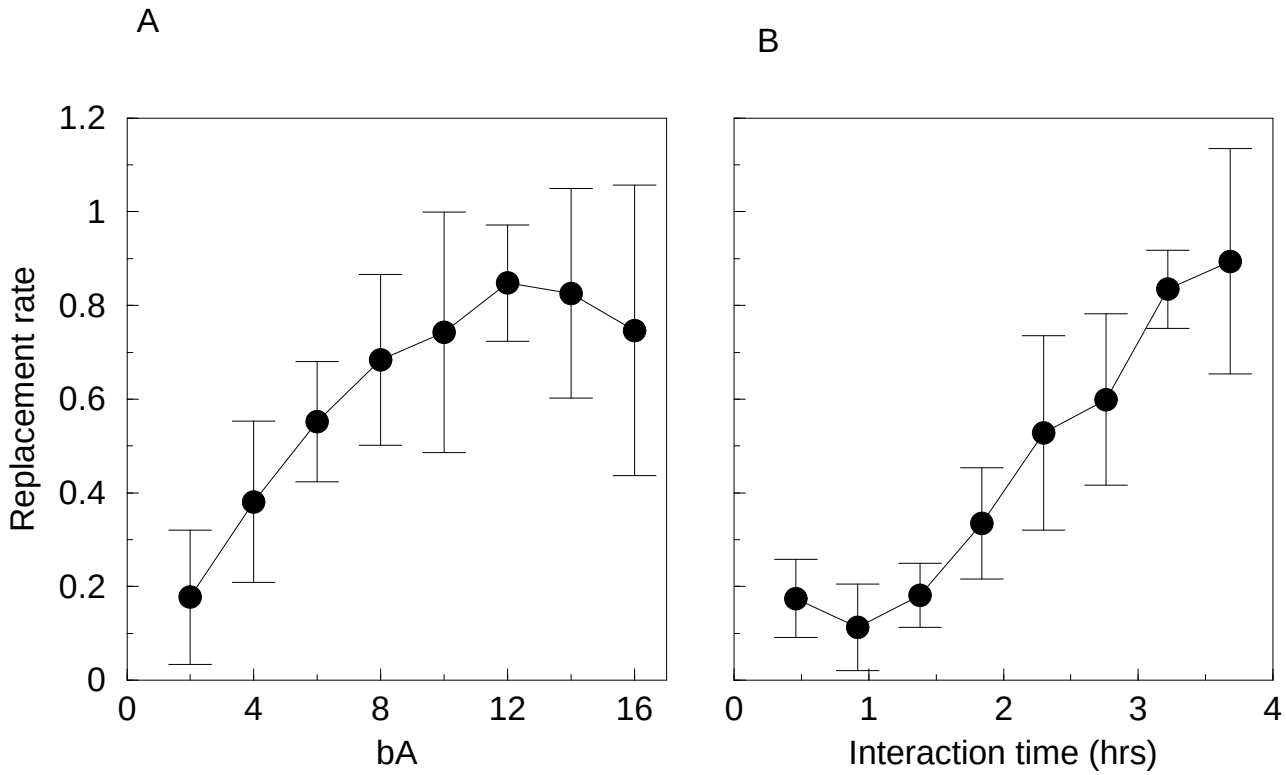
A
B
1.2
1
0.8
0.6
0.4
0.2
0
Replacement rate
0
4
8
12
16
bA
0
1
2
3
4
Interaction time (hrs)

Figure 7: